

## MRI of localized prostate cancer: coming of age in the PSA era

Bařış Türkbeý, Marcelino Bernardo, Maria J. Merino, Bradford J. Wood, Peter A. Pinto, Peter L. Choyke

### ABSTRACT

Prostate cancer is the most common cancer among American men. It varies widely in aggressiveness, ranging from completely indolent to highly aggressive. Currently, predicting the natural history of a particular tumor and deciding on the appropriate treatment, which might include active surveillance, surgery, radiation or hormonal therapies, are based on the condition and age of the patient as well as the presumed stage of the disease. Imaging plays an important role in staging localized prostate cancer. Magnetic resonance imaging (MRI) best depicts the zonal anatomy, with a superior soft tissue resolution providing better results for tumor localization, monitoring, and local staging. Previously, the major function of prostate MRI has been in staging, and this role remains important. In this article, we introduce the reader to the expanding roles that MRI plays in the management of localized prostate cancer.

**Key words:** • prostate cancer • magnetic resonance imaging  
• prostate specific antigen

**P**rostate cancer is the most common cancer among American men, with 217 730 estimated new cases and 32 050 deaths expected in 2010 (1). It can be inferred from these statistics that there is extensive variation in the aggressiveness of prostate cancer, which ranges from completely indolent to highly aggressive. Prostate-specific antigen (PSA) screening has led to a marked increase in the number of patients diagnosed with prostate cancer; most are diagnosed with low-grade disease, but many men are diagnosed with advanced disease. Hence, a rising PSA, although it most likely indicates a low-risk tumor, may also be a harbinger of a deadly malignancy. Many men undergo one or more "blind" prostatic biopsies in response to rising PSA values, but it is possible to miss a large tumor if it is outside the usual biopsy template. Thus, a major role of imaging is to help guide biopsies to detect significant lesions that would otherwise be left undetected.

Unfortunately, predicting the natural history of a particular tumor is difficult, except in extreme situations. Decisions regarding treatments, which include active surveillance (AS), surgery, radiation, and hormonal therapies, are based on the condition and age of the patient as well as the presumed stage of the disease with respect to the prostate capsule, lymph nodes, and distant metastases. Imaging plays an important role in staging localized tumors, but it can also be used to monitor patients who elect to follow their tumors with AS and monitor patients who have been treated for recurrence following therapy. Compared to other imaging modalities magnetic resonance imaging (MRI) is best at depicting the zonal anatomy, although it is not routinely recommended. It also has superior soft tissue resolution in distinguishing the peripheral zone (PZ) from the central gland (CG), resulting in higher yields for tumor localization, monitoring, and local staging. Although the traditional role of prostate MRI has been staging, our purpose in this paper is to introduce the reader to the expanding roles played by MRI in the management of localized prostate cancer. In addition, we describe the classic appearances of prostate cancers discovered and monitored by MRI in these settings.

### MRI of the prostate: normal anatomy and prostate cancer

The basic prostate MRI begins with the placement of an endorectal coil (ERC) following a digital rectal examination (DRE) and involves the acquisition of T2-weighted (T2W) images, diffusion-weighted images, MR spectroscopy, and dynamic contrast-enhanced (DCE) MRI. Imaging can be performed without an endorectal coil, but the quality is usually markedly reduced, especially in diffusion-weighted (DW) imaging and DCE-MRI. Poor image quality makes MRI much more difficult to interpret. Despite the gain in signal from an ERC, its use is perceived as invasive by patients and radiologists. Although an ERC is still considered mandatory for many patients, new phased array coil designs and pulse

From the Molecular Imaging Program (B.T.✉ [bturkbe@yahoo.com](mailto:bturkbe@ yahoo.com), P.L.C.), the Laboratory of Pathology (M.J.M.), and the Urologic Oncology Branch (P.A.P.), National Cancer Institute, NIH, Bethesda, MD, USA; SAIC-Frederick (M.B.), NCI, Frederick, MD, USA; the Center for Interventional Oncology (B.J.W.), NCI; and Radiology and Imaging Sciences, Clinical Center, NIH, Bethesda, MD, USA.

Received 15 April 2011; revision requested 27 May 2011; revision received 31 May 2011; accepted 6 June 2011.

Published online 16 September 2011  
DOI 10.4261/1305-3825.DIR.4478-11.1

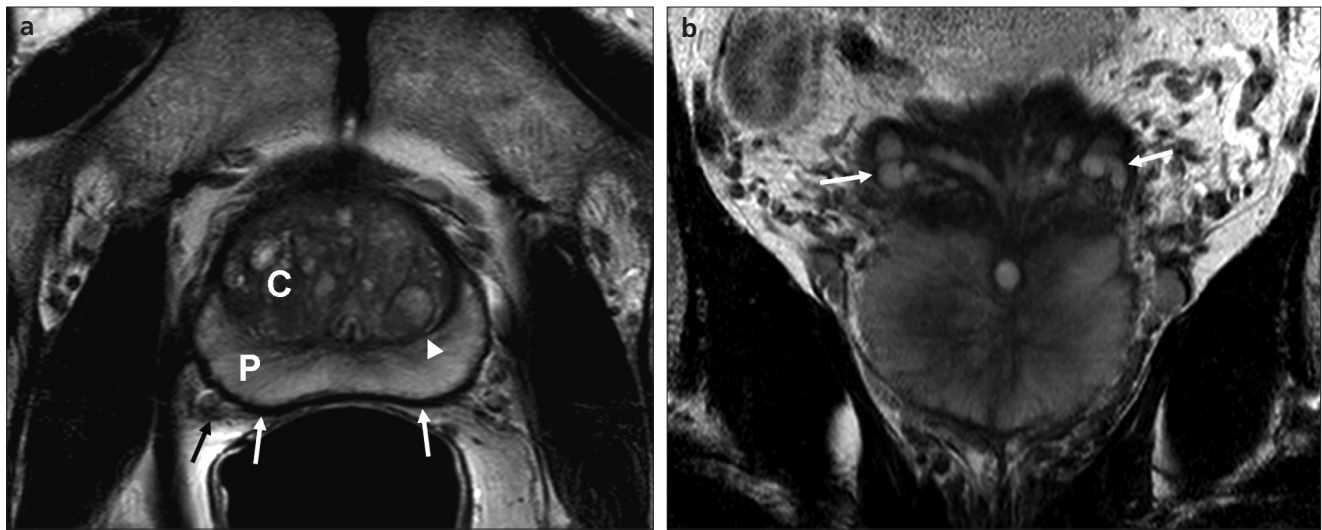


**Figure 1.** **a, b.** Normal prostate anatomy. Axial T2W MR image (**a**) demonstrates a normal peripheral zone (P) that is hyperintense compared to the central gland (C) and is separated by a pseudocapsule (arrowhead); the true capsule of the prostate is seen as a hypointense rim (white arrows) with neurovascular bundles (black arrow); coronal T2W MR image (**b**) shows the seminal vesicles (white arrows) superior to the base of the prostate.

sequences are alternatives that yield comparable image quality.

Anatomically, the prostate can be divided into the peripheral zone and central gland (including the transitional and central-periurethral zones). The normal PZ appears high in signal on T2W MRI, whereas a normal CG has a lower and more heterogeneous signal intensity. The CG is separated from the PZ by a pseudocapsule or surgical capsule. The true capsule, a hypointense rim surrounding the PZ, defines the limits of the prostate and is the site of extracapsular extension. The neurovascular bundles, critical for erectile function, are located at approximately 5 and 7 o'clock posterolateral to the true capsule. The seminal vesicles appear as hyperintense thin-walled cystic structures on T2W MRI, whereas the more medial paired vas deferens are thick-walled and hypointense and can mimic seminal vesicle invasion (Fig. 1). Lymph nodes draining the prostate can be found in the obturator fossa and the peri-rectal space, and higher in the midline of the retroperitoneum.

Prostate cancers usually arise in the PZ and appear as round or ill-defined low-signal-intensity foci on T2W MR images. Detecting tumors in the CG is more complex because the CG becomes progressively larger and more heterogeneous with age; CG tumors are defined as homogenous, low-signal-intensity lesions with irregular margins and without a capsule. They often invade the pseudocapsule or

appear lenticular with extensions into the urethra or anterior fibromuscular zone (2, 3). On DW-MRI, prostate cancers are high in signal due to reduced diffusion, whereas on apparent diffusion coefficient (ADC) maps, they are low in signal intensity (2). On MR spectroscopy, elevated choline levels and/or an elevated ratio of choline to citrate are indicators of prostate cancer (4). On DCE-MRI, prostate cancer usually shows early, rapid enhancement and early washout (5).

#### Clinical roles of prostate MRI

##### *MRI for local staging after a “positive” TRUS-guided biopsy*

As an example, we will follow the typical course of a patient with a rising PSA but no definable lesion on their DRE. Such patients undergo 6–24 systematic core biopsies under transrectal ultrasound guidance (Fig. 2). Patients with an abnormal DRE and/or rising serum PSA usually undergo transrectal ultrasonography (TRUS) guided prostate biopsy, the accepted “gold standard” for diagnosis. The main limitation of the TRUS-guided biopsy is that only a small percentage of the gland is sampled. The lateral PZ may be oversampled, while the midline, antero-lateral, and anterior aspects of the prostate and the CG may be undersampled. The size, location, and extent of the tumor can influence decision making and are generally unknown on the basis of the biopsy alone. Therefore, such patients can be evaluated with an ERC MRI to

determine the size of the tumor. The size or location of the lesion seen on MRI can trigger an additional guided biopsy. For instance, if the initial biopsy suggests a “minimal cancer”, but the MRI identifies a large mass, the patient may then be re-biopsied to obtain a more representative sample (Fig. 3). Prostate cancer is a multifocal, and biologically and histologically heterogeneous disease, which can easily lead to sampling errors (6). Staging by MRI involves visualizing the size and location of the tumor, and the status of the prostate capsule (Fig. 4), seminal vesicles, bladder wall, and local lymph nodes (Fig. 5) (7–21). It should be noted, however, that MRI generally underestimates nodal involvement because it relies on nodal enlargement. The use of MRI for local staging after a “positive” TRUS-guided biopsy constitutes approximately 48% of the total referrals at our center.

##### *MRI for screening before a TRUS-guided biopsy*

A recent debate on the clinical application of prostate MRI centers on whether it can be used as a screening tool before systematic prostate biopsies in patients with an elevated PSA and an abnormal DRE (Fig. 2). Shimizu et al. (22) have recently reported that MRI before a biopsy resulted in a higher rate of prostate cancer detection in 122 patients who underwent T2W MRI and DW-MRI with only a 4-channel external phased array coil. The investigators argue that the use

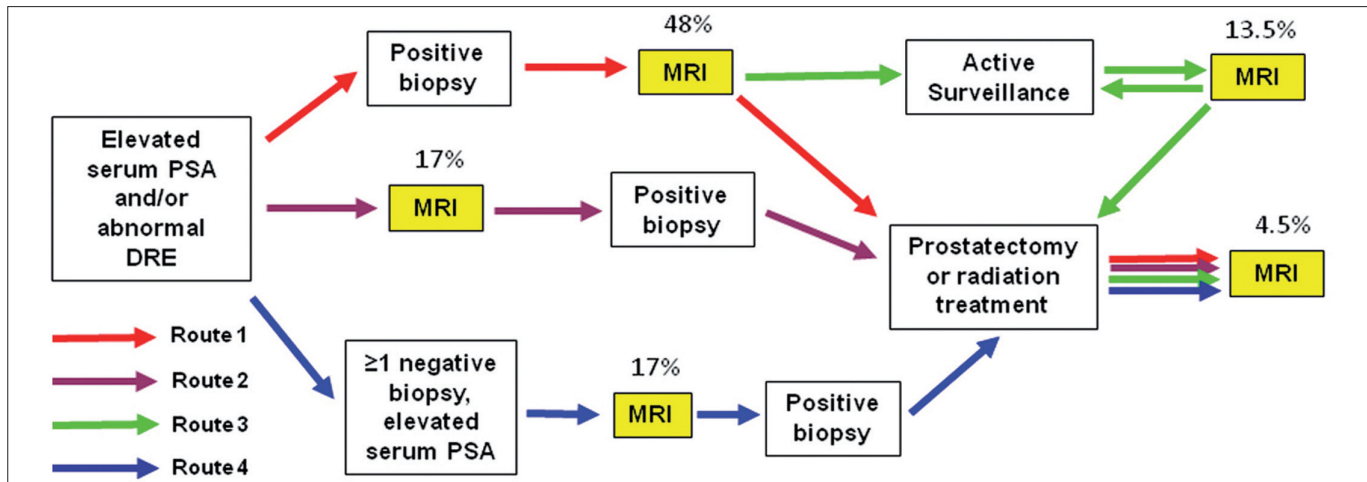


**Figure 2.** Flowchart demonstrating the use of prostate MRI in several clinical scenarios. Route 1 (red) represents the current most common clinical use of MRI as a local staging tool after a positive biopsy and before treatment. Route 2 (purple) represents its use as a “screening tool” before biopsy. Route 3 (green) depicts its role as a “monitoring tool” in active surveillance. Route 4 (blue) represents its use as a “guidance tool” for patients with previous negative biopsies but rising serum PSA. Percentages denote the referral rate of each route on a per patient basis. PSA, prostate-specific antigen; DRE, digital rectal examination.

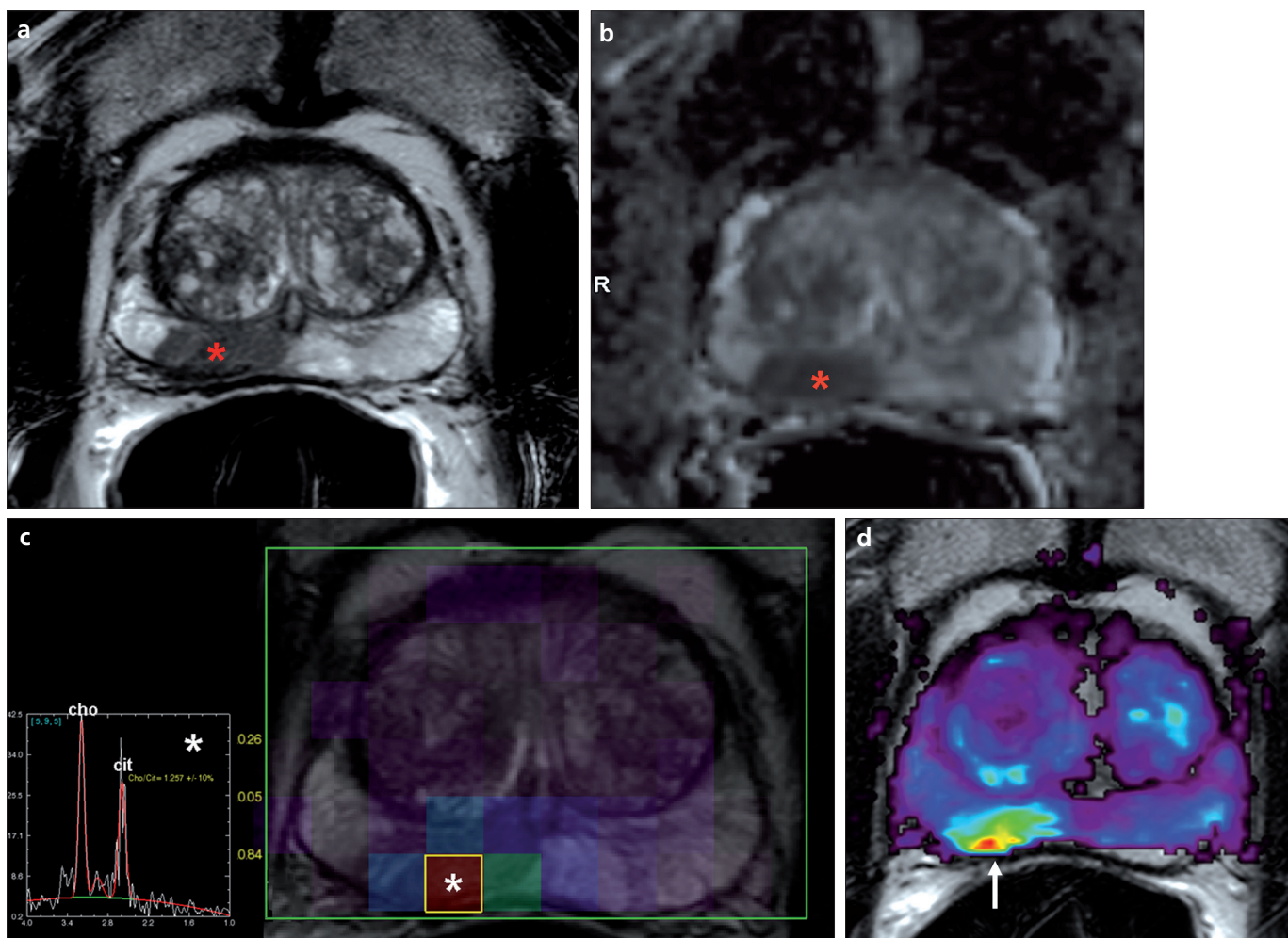


**Figure 3.** a–d. Images from a 59-year-old patient with serum PSA of 8.71 ng/dL and a Gleason-score 3+3 (15% of core) tumor at the right base PZ detected by TRUS-guided biopsy prior to MRI. The axial T2W MR image (a) shows a hypointense lesion in the right mid-base peripheral zone (red asterisk); an ADC map of DW-MRI (b) shows restricted diffusion as a hypointense focus (red asterisk); MR spectroscopy (c) demonstrates an increased choline/citrate ratio within the lesion (white asterisks); and a quantitative map (d) obtained from DCE-MRI localizes the tumor (arrow). The patient underwent a TRUS-MRI-fusion-guided biopsy after MRI, and the right mid-base peripheral zone lesion was found to be upstaged to a Gleason-score 4+4 (90% of core) prostate cancer.

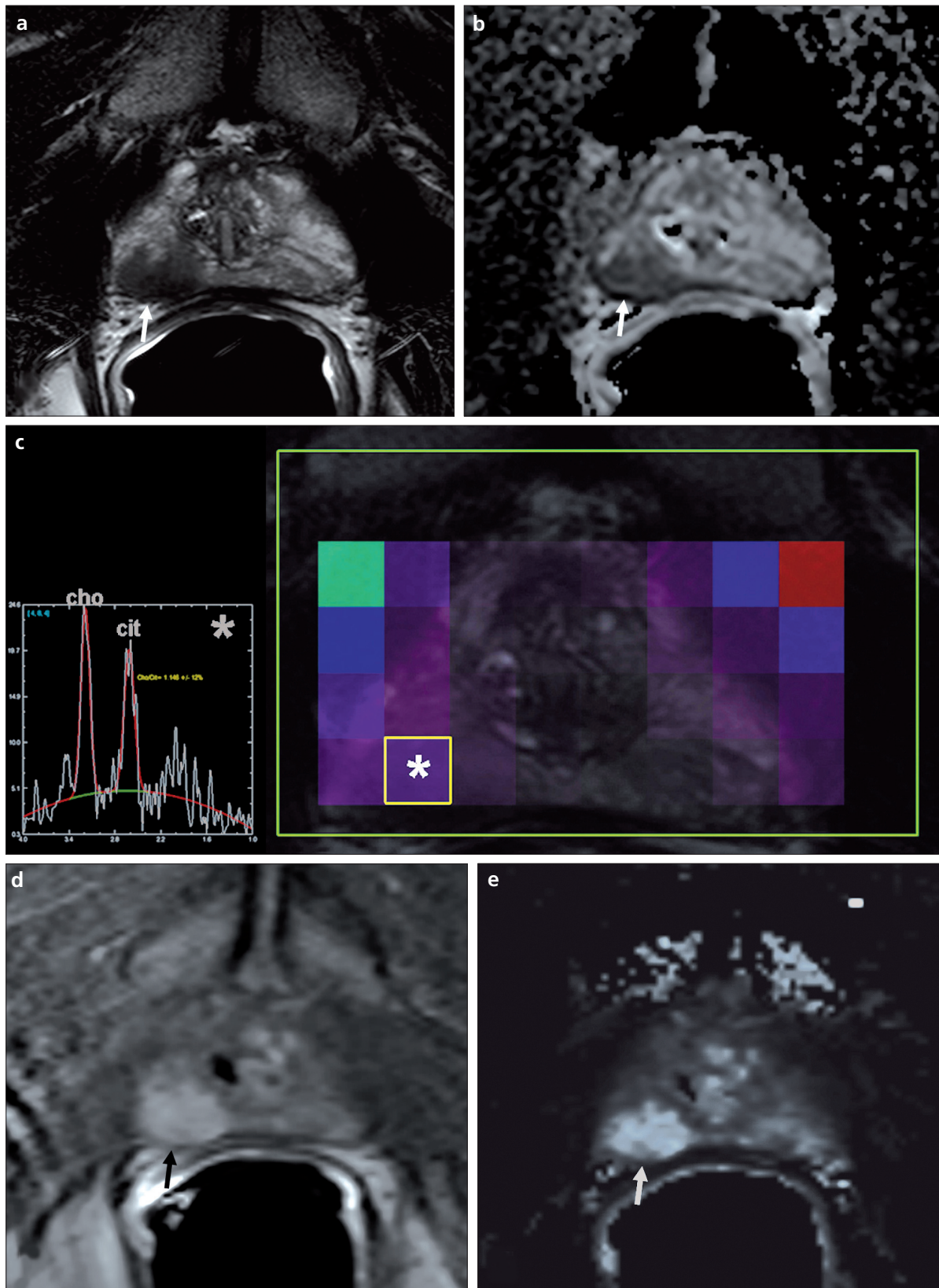


**Figure 4.** a–e. Images from a 57-year-old patient with a PSA of 3.35 ng/dL and a Gleason-score 3+4 (70% of core) tumor at the right apical peripheral zone, detected by a TRUS-guided biopsy prior to MRI. The axial T2W MR image (a) shows a hypointense lesion in the right apical peripheral zone with extracapsular extension (arrow); an ADC map of DW-MRI (b) shows restricted diffusion as a hypointense focus (arrow) corresponding to the right apical peripheral zone lesion; MR spectroscopy (c) demonstrates an increased choline/citrate ratio within the lesion (white asterisk); and a raw DCE-MRI image (d) and quantitative map (e) obtained from DCE-MRI localize the tumor (arrows in d and e).

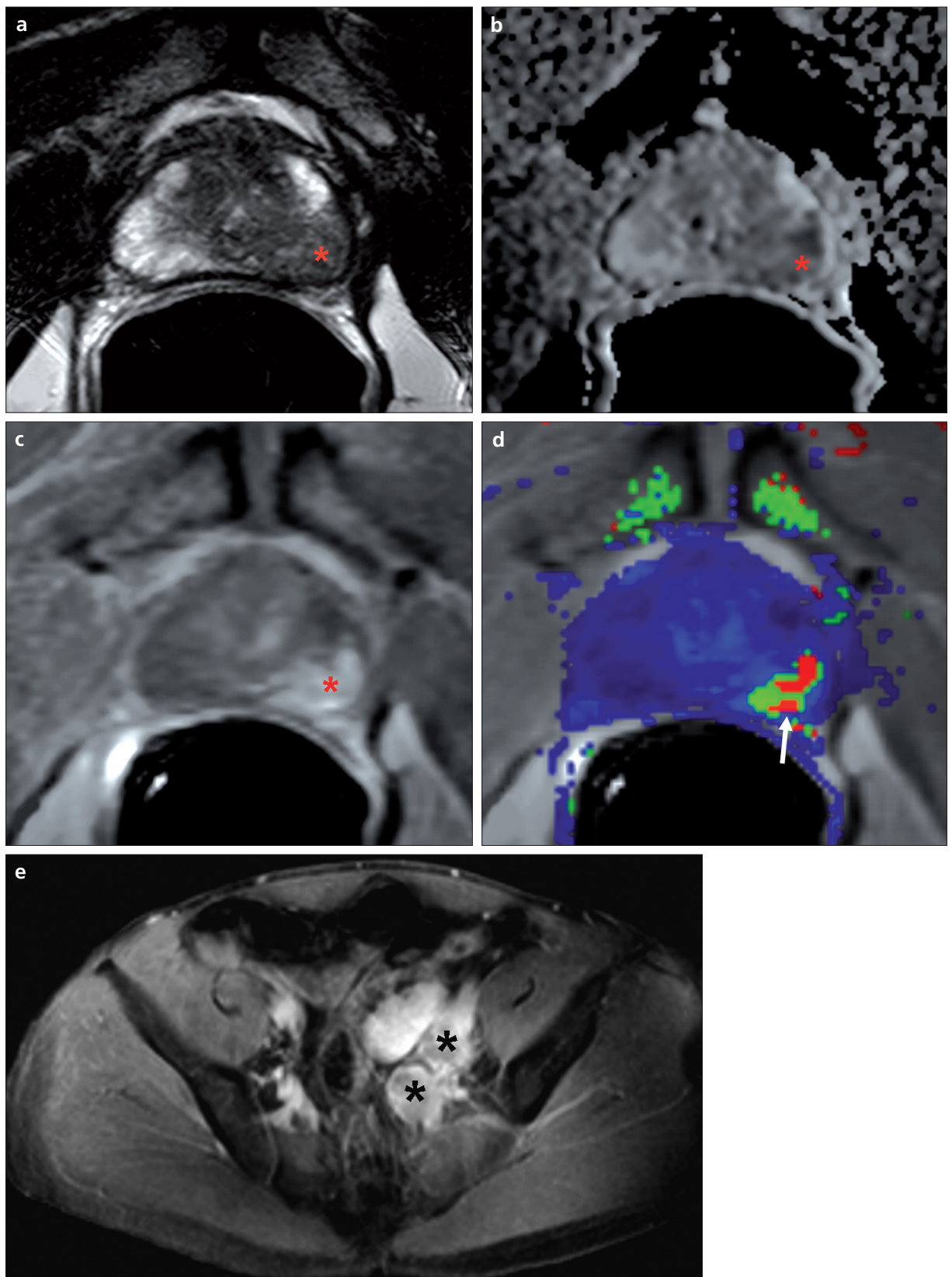


**Figure 5.** a–e. Images from a 43-year-old patient with a PSA of 30 ng/dL. The axial T2W MR image (a) shows a hypointense lesion in the left apical peripheral zone (red asterisk); an ADC map of DW-MRI (b) shows restricted diffusion as a hypointense focus (red asterisk) corresponding to the left apical peripheral zone lesion; the raw DCE-MR image (c) and the quantitative map (d) obtained from DCE-MRI localize the tumor (red asterisk in c, arrow in d); and an axial contrast-enhanced T1W image of the pelvis (e) shows an enlarged left iliac lymph node secondary to prostate cancer metastases (black asterisks).

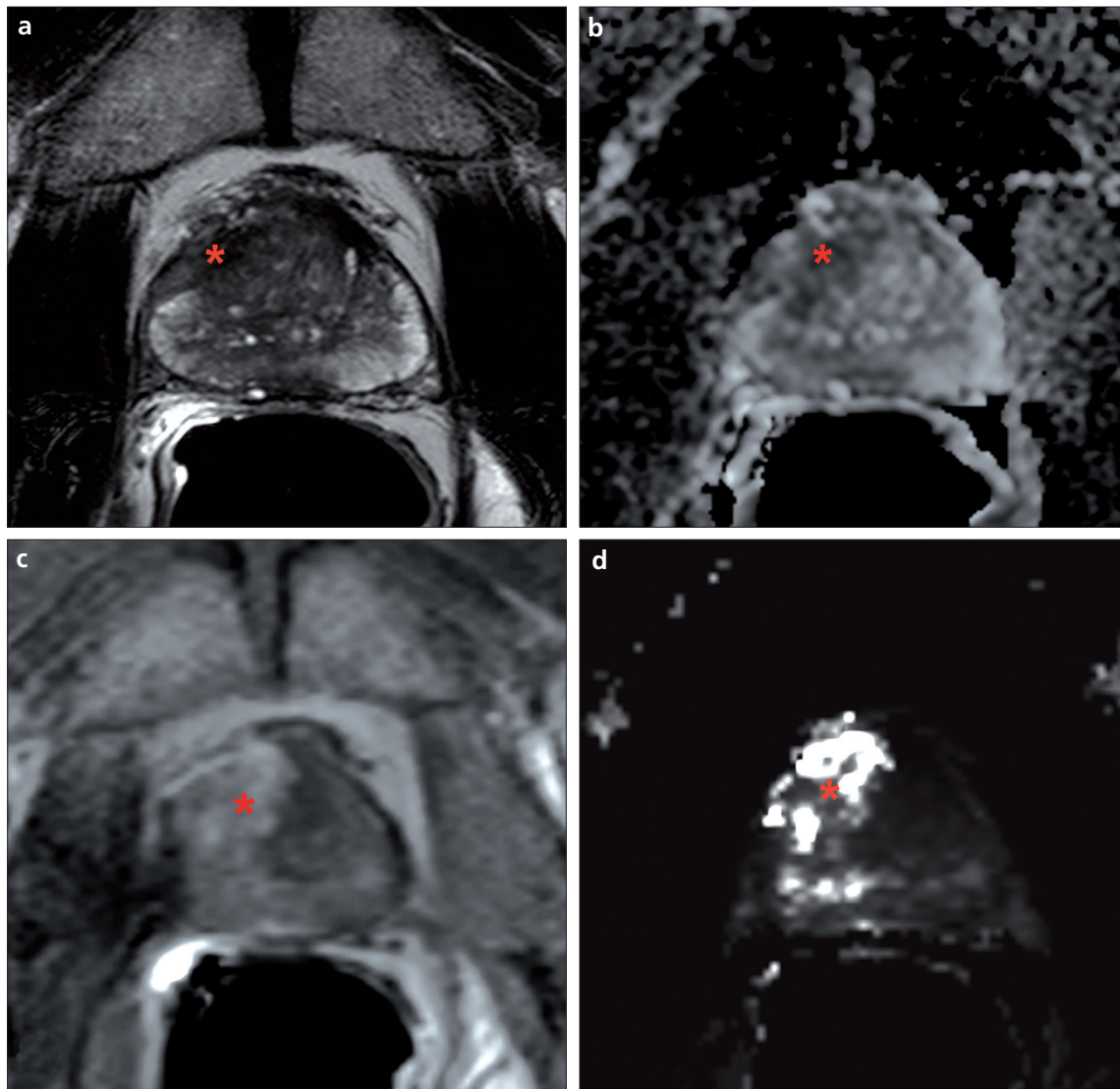


**Figure 6.** a-d. Images from a 50-year-old patient with a serum PSA of 15.8 ng/dL without any prior prostate biopsy history. The axial T2W MR image (a) shows a hypointense lesion in the right mid-base anterior central gland (red asterisk); an ADC map of DW-MRI (b) shows restricted diffusion within the lesion (red asterisk); and a raw DCE-MRI image (c) and the quantitative map (d) obtained from DCE-MRI demonstrate early and fast enhancement within the lesion (red asterisks). The patient underwent TRUS-MRI-fusion-guided prostate biopsy, and the right mid-base anterior central gland lesion was found to contain Gleason-score 4+5 (100% of core) prostate cancer.

of MRI data during biopsies (e.g., TRUS-MRI fusion for guidance) can potentially decrease the number of patients undergoing unnecessary prostate biopsies and increase the yield of those who do, but the cost-effectiveness of this approach has not been demonstrated (23) (Fig. 6). Some patients, recognizing the “blind” nature of routine biopsies, request ERC MRIs before their first biopsy. Referrals to MRI for pre-biopsy screening constitute approximately 17% of total referrals in our practice.

#### *MRI as a roadmap after one or more “negative” TRUS-guided biopsies*

Patients with negative biopsies return to the screening pool (Fig. 2). If

their PSA levels continue to rise after a negative biopsy, the next step in patient management becomes challenging, especially considering that up to 90% of patients have a negative result after an initial negative biopsy (24, 25). One option for such cases is the saturation biopsy, which may include obtaining 100 or more cores; however, this procedure can result in complications such as urinary retention, hematuria and sepsis, and is costly due to multiple specimen processing and interpretation (26). Another approach is to use MRI to localize suspicious areas for biopsy, especially if the lesion is in the anterior and CG lesions, the site of approximately 20%-30% of all

prostate cancers (27, 28). An MRI scan at this point may direct the biopsy to an area that would not ordinarily be sampled (Fig. 7). Recently, MRI in patients with persistently elevated PSA and one or more prior negative prostate biopsies was reported to increase tumor detection rate by 25%-45% on a per-patient basis (29-32). In addition to using MR images as a virtual guide for repeat biopsies, the biopsy procedure can be performed under real-time MRI guidance or potentially combined with real-time TRUS to guide repeat biopsies (33, 34). MRI has been used as a problem-solving tool following “negative” and “inconclusive” biopsies in 17% of our prostate MRI referrals.

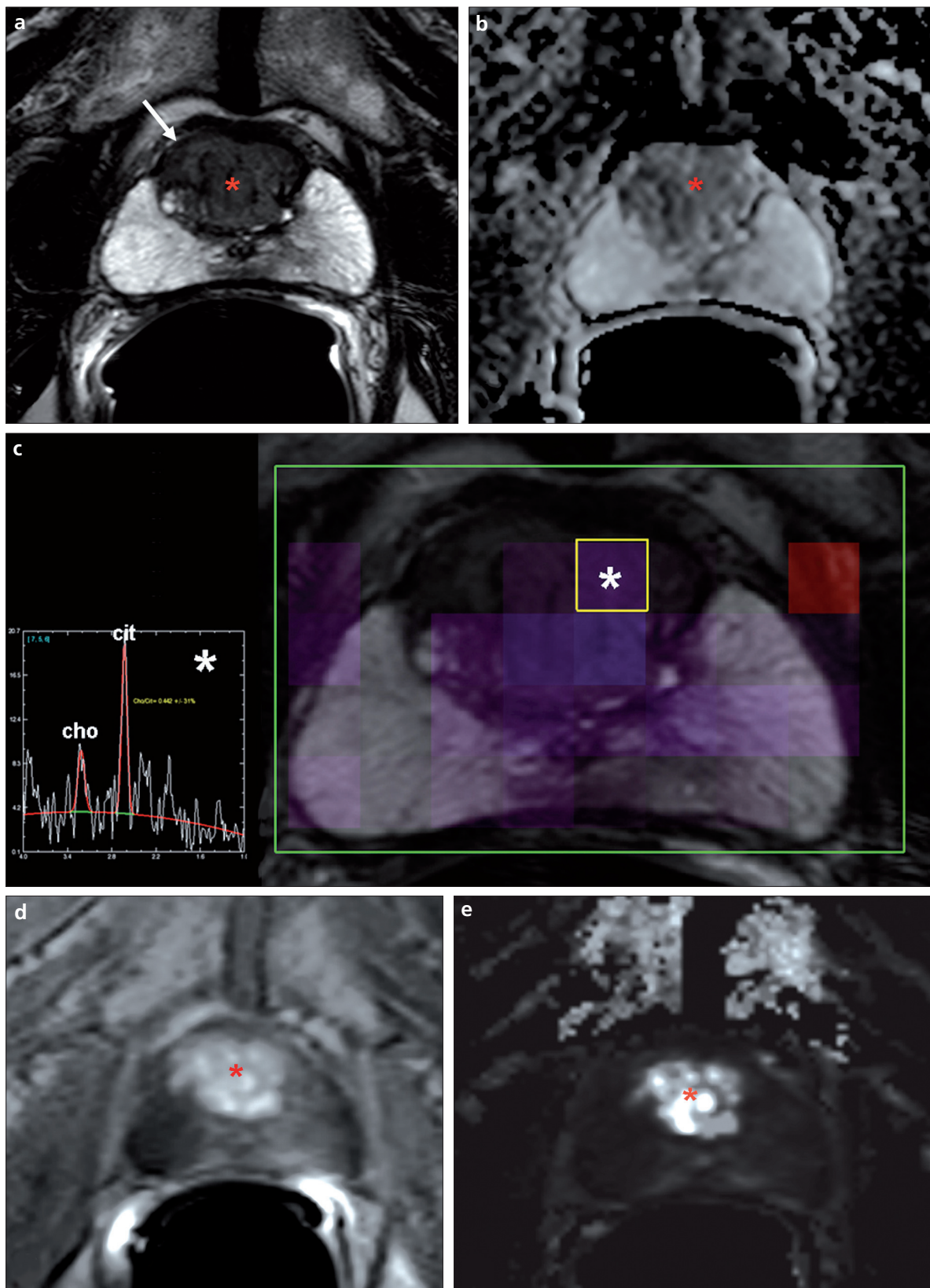


**Figure 7.** a–e. Images from a 67-year-old patient with a serum PSA of 21.4 ng/dL with seven negative TRUS-guided prostate biopsies prior to MRI. The axial T2W MR image (a) shows a hypointense lesion in the mid-anterior central gland (arrow and red asterisk); an ADC map of DW-MRI (b) shows restricted diffusion within the lesion (red asterisk); MR spectroscopy (c) demonstrates an increased choline/citrate ratio within the lesion (white asterisks); and a raw DCE-MRI image (d) and the quantitative map (e) obtained from DCE-MRI demonstrate early and fast enhancement within the lesion (red asterisk). The patient underwent TRUS-MRI-fusion-guided prostate biopsy, and the mid-anterior central gland lesion was found to contain Gleason-score 3+4 (70% of core) prostate cancer.

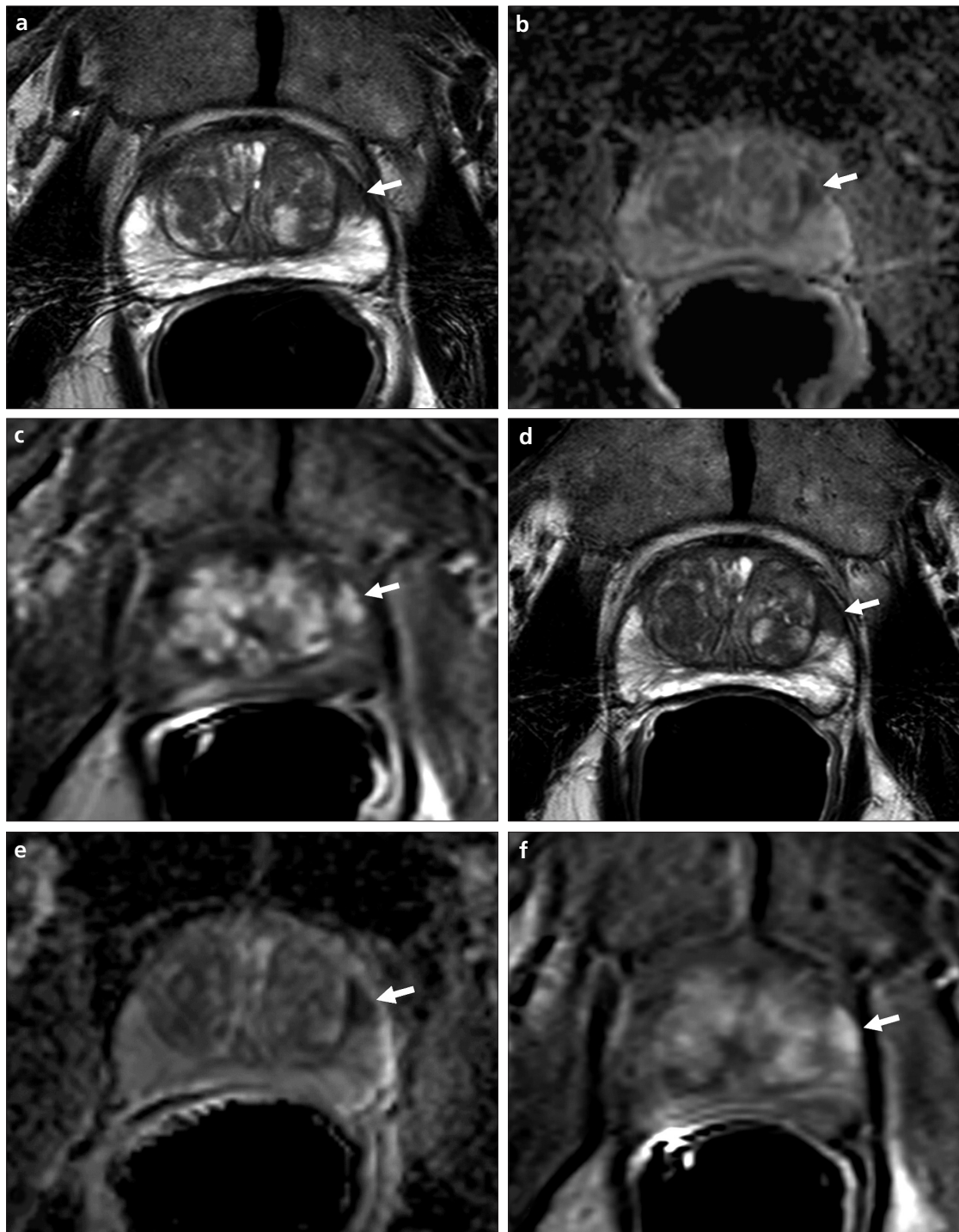


**Figure 8.** a-f. Images from a 82-year-old patient with a serum PSA of 4.9 ng/dL on active surveillance for a Gleason-score 3+4 (50% of core) tumor at the left mid-peripheral zone. The axial T2W MR image (a) shows a hypointense lesion in the left mid-anterior peripheral zone (arrow); an ADC map of DW-MRI (b) shows restricted diffusion within the lesion (arrow); and a raw DCE-MRI image (c) demonstrates focal hyperenhancement within the lesion (arrow). One-year follow-up T2W MR images (d), ADC maps of DW-MRI (e), and DCE-MRI (f) demonstrate no change in MR imaging findings (arrows).

#### *MRI as a monitoring tool for active surveillance*

Because prostate cancer exists as a spectrum of pathologies that range from indolent to highly aggressive, and patients with indolent cancers may not require radical prostatectomy or radiation therapy, AS is often suggested for patients with low-volume and clinically low-risk disease (35–38). Multiparametric MRI,

including T2W MRI, DW-MRI, MR spectroscopy, and DCE-MRI, can potentially help to correctly stratify such patients in the pretreatment phase because it may help predict patterns of tumor growth and thus identify the prognosis (39–46).

Studies have suggested that AS may be an alternative to radical therapies for carefully selected patients (47, 48). AS is an emerging methodology that

involves serial PSA measurements and annual biopsies, and it has not been standardized (49, 50). A few large-scale clinical studies have recently reported favorable outcomes using AS of prostate cancer (51, 52). Lesions eligible for AS can be depicted by multiparametric MRI and tracked, allowing tumors that transform to a more aggressive phenotype to be identified (53, 54) (Figs. 8 and 9). The AS patient

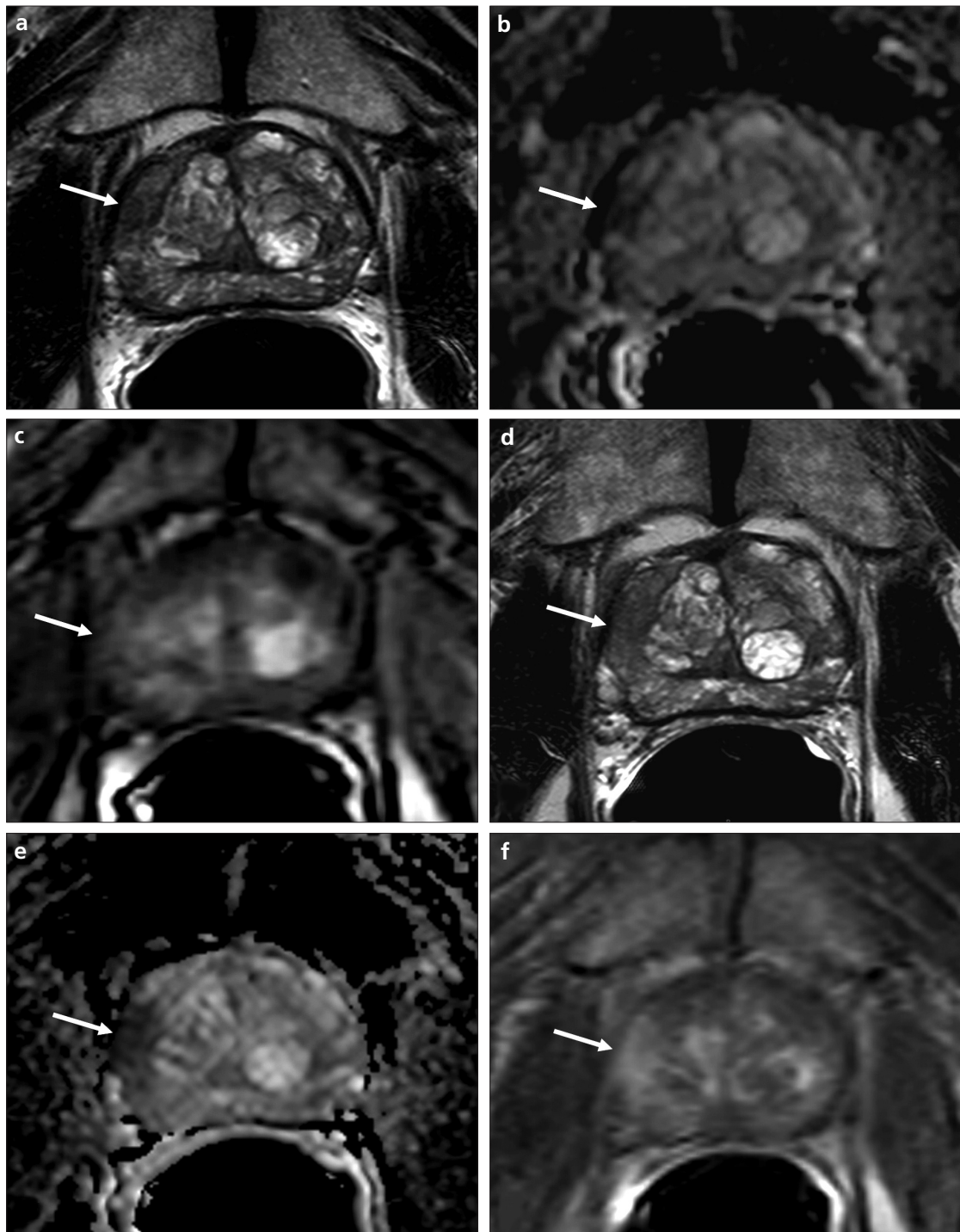


**Figure 9.** a-f. Images from a 72-year-old patient with a serum PSA of 4.96 ng/dL on active surveillance for a Gleason-score 3+3 (30% of core) tumor at the right mid-peripheral zone. The axial T2W MR image (a) shows a hypointense lesion in the right mid-anterior peripheral zone (arrow); an ADC map of DW-MRI (b) shows restricted diffusion within the lesion (arrow); and a raw DCE-MRI image (c) demonstrates focal hyper-enhancement within the lesion (arrow). The first-year follow-up T2W MR image (d), ADC map of DW-MRI (e), and DCE-MRI (f) demonstrate a slight increase in lesion size (arrows). The serum PSA of the patient also increased to 7.9 ng/dL in the interval, and a repeat TRUS-MRI-fusion-guided biopsy after follow-up MRI revealed a Gleason-score 3+3 (50% of core) tumor in the right mid-anterior peripheral zone.

population constitutes 13.5% of prostate MRI referrals in our practice.

#### *MRI as a monitoring tool for treatment follow-up*

The treatment options for patients with prostate cancer include radical prostatectomy (RP), hormone therapy, radiation therapy (e.g. external beam radiation and brachytherapy) and focal therapy (radiofrequency ablation,

cryotherapy, high-intensity focus ultrasound, and cyberknife). Selection of the optimal treatment method is based on clinical tumor stage, Gleason score, PSA level, and other factors such as patient age, condition and other comorbidities. Patients are followed by serum PSA and DRE after treatment for prostate cancer. MRI can play a role in detecting local recurrence when PSA begins to rise after anadir. For instance,

biochemical relapse after RP can occur in 15%-30% of patients (55-58). Currently, clinical nomograms are used to predict the risk of biochemical recurrence; however, these nomograms have some limitations related to their variables, such as the low specificity of serum PSA and underestimated Gleason score at biopsy. MRI has been shown to improve the detection of local recurrence in patients with RP in

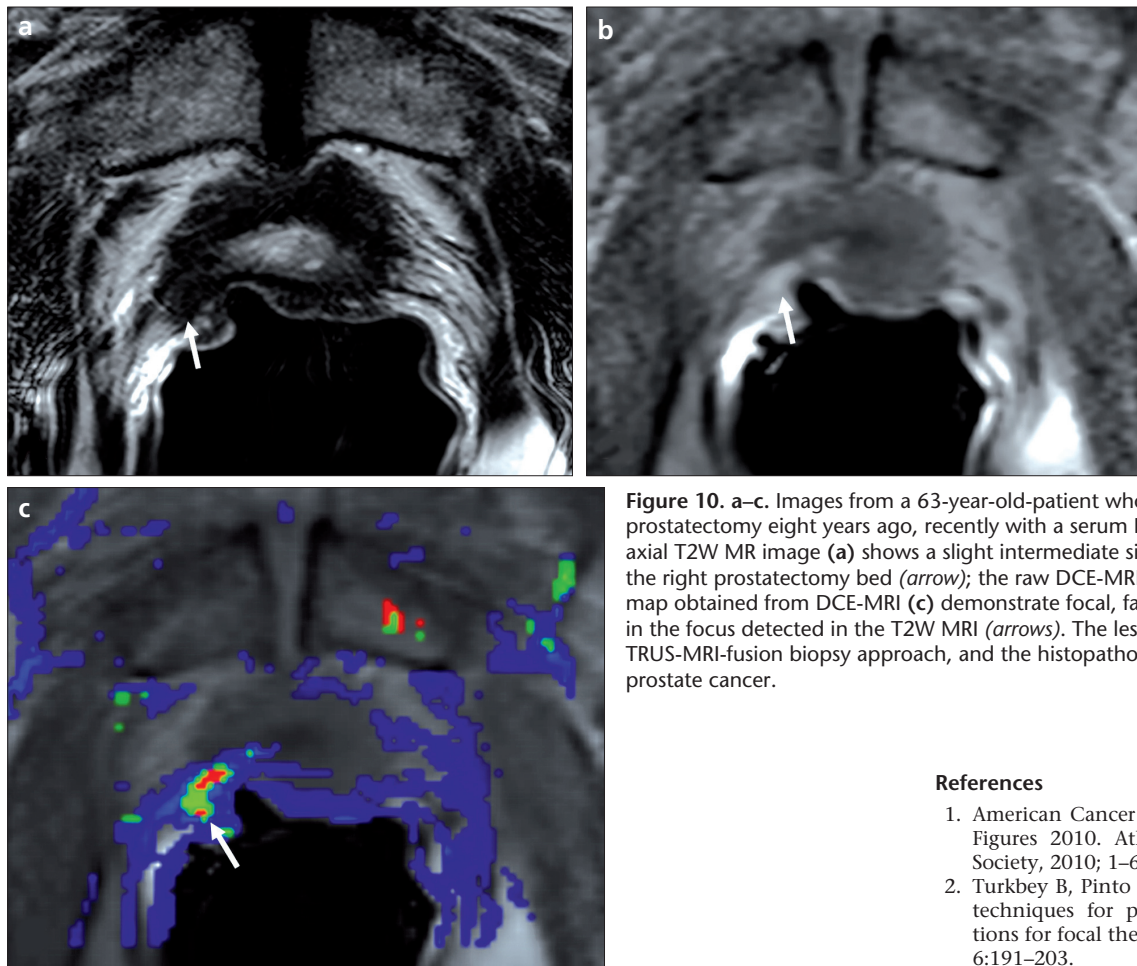


**Figure 10.** a–c. Images from a 63-year-old-patient who had a radical prostatectomy eight years ago, recently with a serum PSA of 0.59 ng/dL. The axial T2W MR image (a) shows a slight intermediate signal-intensity focus in the right prostatectomy bed (arrow); the raw DCE-MRI (b) and quantitative map obtained from DCE-MRI (c) demonstrate focal, fast hyper-enhancement in the focus detected in the T2W MRI (arrows). The lesion was sampled via the TRUS-MRI-fusion biopsy approach, and the histopathology revealed recurrent prostate cancer.

## References

- American Cancer Society. *Cancer Facts & Figures 2010*. Atlanta: American Cancer Society, 2010; 1–63.
- Turkbey B, Pinto PA, Choyke PL. Imaging techniques for prostate cancer: implications for focal therapy. *Nat Rev Urol* 2009; 6:191–203.
- Akin O, Sala E, Moskowitz CS, et al. Transition zone prostate cancers: features, detection, localization, and staging at endorectal MR imaging. *Radiology* 2006; 239:784–792.
- Kurhanewicz J, Vigneron DB, Hricak H, Narayan P, Carroll P, Nelson SJ. Three-dimensional H-1 MR spectroscopic imaging of the *in situ* human prostate with high (0.24–0.7-cm<sup>3</sup>) spatial resolution. *Radiology* 1996; 198:795–805.
- Ocak I, Bernardo M, Metzger G, et al. Dynamic contrast-enhanced MRI of prostate cancer at 3 T: a study of pharmacokinetic parameters. *AJR Am J Roentgenol* 2007; 189:849.
- Punglia RS, D'Amico AV, Catalona WJ, Roehl KA, Kuntz KM. Effect of verification bias on screening for prostate cancer by measurement of prostate-specific antigen. *N Engl J Med* 2003; 349:335–342.
- Zhang J, Hricak H, Shukla-Dave A, et al. Clinical stage T1c prostate cancer: evaluation with endorectal MR imaging and MR spectroscopic imaging. *Radiology* 2009; 253:425–434.
- Villeirs GM, De Meerleer GO, De Visschere PJ, Fonteyne VH, Verbaeys AC, Oosterlinck W. Combined magnetic resonance imaging and spectroscopy in the assessment of high grade prostate carcinoma in patients with elevated PSA: a single-institution experience of 356 patients. *Eur J Radiol* 2011; 77:340–345.

a few studies (59–60). Although it is challenging to detect local recurrence on T2W MR images, the combined use of T2W MRI with DCE-MRI results in a higher yield in detecting local recurrence (61) (Fig. 10).

External-beam radiation therapy (EBRT) is employed in approximately one-third of prostate cancer patients, and biochemical recurrence can occur in 20%–40% in the first five years (62). Detecting recurrence after EBRT can be challenging because the PSA level may not be a reliable marker, and the DRE can be non-specific due to atrophic and fibrotic changes in the irradiated prostate gland. Multi-parametric MRI, specifically MR spectroscopy and DCE-MRI, can help identify recurrences with high accuracy in post-radiotherapy patients (63–66). Post-treatment follow-up comprises 4.5% of prostate MRI referrals. Similar comments apply to focal therapies such as focal cryotherapy and high-intensity focused ultrasound (Fig. 11).

Among the available imaging modalities, MRI currently provides the most valuable anatomic and functional information about the prostate gland. Although MRI yielded disappointing results when used in staging, its role has expanded with changes in how prostate cancer is perceived, treated and followed. MRI is currently mostly used for localization and local staging in prostate cancer patients who are surgery or radiation candidates. However, in addition to its traditional roles, MRI is being used as a monitoring tool in AS and in RP and post-radiation patients; it is also used to help diagnose patients with negative prior biopsies but rising PSA (Fig. 2). Prostate MRI has come of age in the PSA era.

## Conflict of interest disclosure

The authors declared no conflicts of interest.

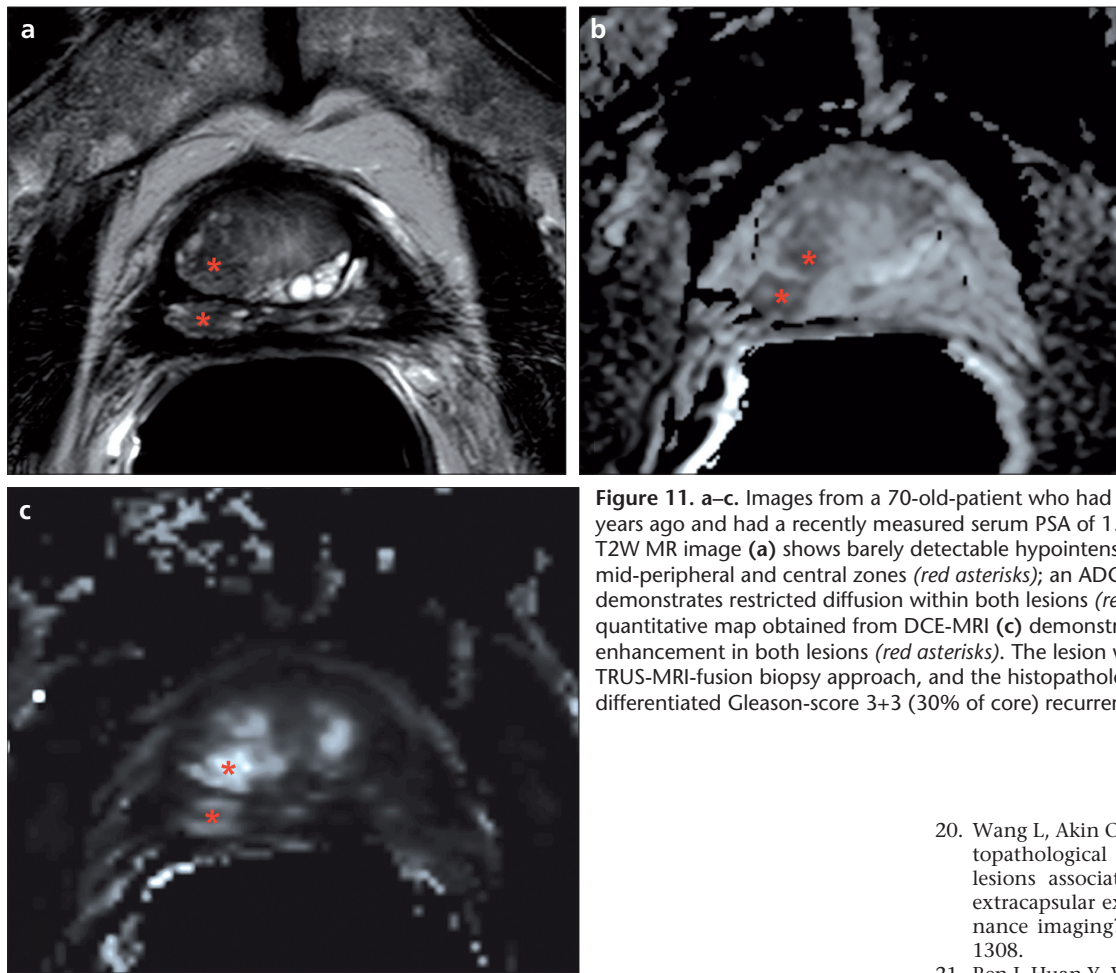


**Figure 11.** a–c. Images from a 70-old-patient who had focal cryoablation two years ago and had a recently measured serum PSA of 1.57 ng/dL. The axial T2W MR image (a) shows barely detectable hypointense lesions in the right mid-peripheral and central zones (red asterisks); an ADC map of DW-MRI (b) demonstrates restricted diffusion within both lesions (red asterisks); and a quantitative map obtained from DCE-MRI (c) demonstrates focal, fast hyperenhancement in both lesions (red asterisks). The lesion was sampled via the TRUS-MRI-fusion biopsy approach, and the histopathology revealed moderately differentiated Gleason-score 3+3 (30% of core) recurrent prostate cancer.

9. Turkbey B, Pinto PA, Mani H, et al. Prostate cancer: value of multiparametric MR imaging at 3 T for detection–histopathologic correlation. *Radiology* 2010; 255:89–99.
10. Vilanova JC, Comet J, Barceló-Vidal C, et al. Peripheral zone prostate cancer in patients with elevated PSA levels and low free-to-total PSA ratio: detection with MR imaging and MR spectroscopy. *Radiology* 2009; 253:135–143.
11. Puech P, Potiron E, Lemaitre L, et al. Dynamic contrast-enhanced-magnetic resonance imaging evaluation of intraprostatic prostate cancer: correlation with radical prostatectomy specimens. *Urology* 2009; 74:1094–1099.
12. Lawrentschuk N, Haider MA, Daljeet N, et al. ‘Prostatic evasive anterior tumours’: the role of magnetic resonance imaging. *BJU Int* 2010; 105:1231–1236.
13. Yağcı AB, Ozari N, Aybek Z, Düzcan E. The value of diffusion-weighted MRI for prostate cancer detection and localization. *Diagn Interv Radiol* 2011; 17:130–134.
14. Iwazawa J, Mitani T, Sassa S, Ohue S. Prostate cancer detection with MRI: is dynamic contrast-enhanced imaging necessary in addition to diffusion-weighted imaging? *Diagn Interv Radiol* 2011; 17:243–248.
15. Lim HK, Kim JK, Kim KA, Cho KS. Prostate cancer: apparent diffusion coefficient map with T2-weighted images for detection—a multireader study. *Radiology* 2009; 250:145–151.
16. Riches SF, Payne GS, Morgan VA, et al. MRI in the detection of prostate cancer: combined apparent diffusion coefficient, metabolite ratio, and vascular parameters. *AJR Am J Roentgenol* 2009; 193:1583–1591.
17. Kitajima K, Kaji Y, Fukabori Y, Yoshida K, Sugimura N, Sugimura K. Prostate cancer detection with 3 T MRI: comparison of diffusion-weighted imaging and dynamic contrast-enhanced MRI in combination with T2-weighted imaging. *J Magn Reson Imaging* 2010; 31:625–631.
18. Langer DL, van der Kwast TH, Evans AJ, Trachtenberg J, Wilson BC, Haider MA. Prostate cancer detection with multi-parametric MRI: logistic regression analysis of quantitative T2, diffusion-weighted imaging, and dynamic contrast-enhanced MRI. *J Magn Reson Imaging* 2009; 30:327–334.
19. Labanaris AP, Zugor V, Takriti S, et al. The role of conventional and functional endorectal magnetic resonance imaging in the decision of whether to preserve or resect the neurovascular bundles during radical retropubic prostatectomy. *Scand J Urol Nephrol* 2009; 43:25–31.
20. Wang L, Akin O, Mazaheri Y, et al. Are histopathological features of prostate cancer lesions associated with identification of extracapsular extension on magnetic resonance imaging? *BJU Int* 2010; 106:1303–1308.
21. Ren J, Huan Y, Wang H, et al. Seminal vesicle invasion in prostate cancer: prediction with combined T2-weighted and diffusion-weighted MR imaging. *Eur Radiol* 2009; 19:2481–2486.
22. Shimizu T, Nishie A, Ro T, et al. Prostate cancer detection: the value of performing an MRI before a biopsy. *Acta Radiol* 2009; 50:1080–1088.
23. Xu S, Kruecker J, Turkbey B, et al. Real-time MRI-TRUS fusion for guidance of targeted prostate biopsies. *Comput Aided Surg* 2008; 13:255–264.
24. Djavan B, Raverty V, Zlotta A, et al. Prospective evaluation of prostate cancer detected on biopsies 1, 2, 3 and 4: when should we stop? *J Urol* 2001; 166:1679–1683.
25. Lujan M, Paez A, Santonja C, Pascual T, Fernandez I, Berenguer A. Prostate cancer detection and tumor characteristics in men with multiple biopsy sessions. *Prostate Cancer Prostatic Dis* 2004; 7:238–242.
26. Stewart CS, Leibovich BC, Weaver AL, Lieber MM. Prostate cancer diagnosis using a saturation needle biopsy technique after previous negative sextant biopsies. *J Urol* 2001; 166:86–91.
27. Bott SR, Young MP, Kellett MJ, Parkinson MC; Contributors to the UCL Hospitals’ Trust Radical Prostatectomy Database. Anterior prostate cancer: is it more difficult to diagnose? *BJU Int* 2002; 89:886–889.

28. Bouyé S, Potiron E, Puech P, Leroy X, Lemaitre L, Villers A. Transition zone and anterior stromal prostate cancers: zone of origin and intraprostatic patterns of spread at histopathology. *Prostate* 2009; 69:105–113.
29. Park BK, Lee HM, Kim CK, Choi HY, Park JW. Lesion localization in patients with a previous negative transrectal ultrasound biopsy and persistently elevated prostate specific antigen level using diffusion-weighted imaging at three Tesla before re-biopsy. *Invest Radiol* 2008; 43:789–793.
30. Cirillo S, Petracchini M, Della Monica P, et al. Value of endorectal MRI and MRS in patients with elevated prostate-specific antigen levels and previous negative biopsies to localize peripheral zone tumours. *Clin Radiol* 2008; 63:871–879.
31. Cheikh AB, Girouin N, Colombel M, et al. Evaluation of T2-weighted and dynamic contrast-enhanced MRI in localizing prostate cancer before repeat biopsy. *Eur Radiol* 2009; 19:770–778.
32. Sciarra A, Panebianco V, Ciccarello M, et al. Value of magnetic resonance spectroscopy imaging and dynamic contrast-enhanced imaging for detecting prostate cancer foci in men with prior negative biopsy. *Clin Cancer Res* 2010; 16:1875–1883.
33. Susil RC, Ménard C, Krieger A, et al. Transrectal prostate biopsy and fiducial marker placement in a standard 1.5T magnetic resonance imaging scanner. *J Urol* 2006; 175:113–120.
34. Singh AK, Kruecker J, Xu S, et al. Initial clinical experience with real-time transrectal ultrasonography-magnetic resonance imaging fusion-guided prostate biopsy. *BJU Int* 2008; 101:841–845.
35. D'Amico AV, Whittington R, Malkowicz SB, et al. Biochemical outcome after radical prostatectomy, external beam radiation therapy, or interstitial radiation therapy for clinically localized prostate cancer. *JAMA* 1998; 280:969–974.
36. Partin AW, Mangold LA, Lamm DM, Walsh PC, Epstein JI, Pearson JD. Contemporary update of prostate cancer staging nomograms (Partin Tables) for the new millennium. *Urology* 2001; 58:843–848.
37. D'Amico AV, Moul J, Carroll PR, Sun L, Lubeck D, Chen MH. Cancer-specific mortality after surgery or radiation for patients with clinically localized prostate cancer managed during the prostate-specific antigen era. *J Clin Oncol* 2003; 21:2163–2172.
38. Stephenson AJ, Scardino PT, Eastham JA, et al. Preoperative nomogram predicting the 10-year probability of prostate cancer recurrence after radical prostatectomy. *J Natl Cancer Inst* 2006; 98:715–717.
39. Wang L, Mazaheri Y, Zhang J, Ishill NM, Kuroiwa K, Hricak H. Assessment of biologic aggressiveness of prostate cancer: correlation of MR signal intensity with Gleason grade after radical prostatectomy. *Radiology* 2008; 246:168–176.
40. Zakian KL, Sircar K, Hricak H, et al. Correlation of proton MR spectroscopic imaging with gleason score based on step-section pathologic analysis after radical prostatectomy. *Radiology* 2005; 234:804–814.
41. Wang XZ, Wang B, Gao ZQ, et al. Diffusion-weighted imaging of prostate cancer: correlation between apparent diffusion coefficient values and tumor proliferation. *J Magn Reson Imaging* 2009; 29:1360–1366.
42. Tamada T, Sone T, Jo Y, et al. Apparent diffusion coefficient values in peripheral and transition zones of the prostate: comparison between normal and malignant prostatic tissues and correlation with histologic grade. *J Magn Reson Imaging* 2008; 28:720–726.
43. Zelhof B, Pickles M, Liney G, et al. Correlation of diffusion-weighted magnetic resonance data with cellularity in prostate cancer. *BJU Int* 2009; 103:883–888.
44. deSouza NM, Riches SF, Vanas NJ, et al. Diffusion-weighted magnetic resonance imaging: a potential non-invasive marker of tumour aggressiveness in localized prostate cancer. *Clin Radiol* 2008; 63:774–782.
45. Zakian KL, Hricak H, Ishill N, et al. An exploratory study of endorectal magnetic resonance imaging and spectroscopy of the prostate as preoperative predictive biomarkers of biochemical relapse after radical prostatectomy. *J Urol* 2010; 184:2320–2327.
46. Fradet V, Kurhanewicz J, Cowan JE, et al. Prostate cancer managed with active surveillance: role of anatomic MR imaging and MR spectroscopic imaging. *Radiology* 2010; 256:176–183.
47. Dall'Era MA, Konety BR, Cowan JE, et al. Active surveillance for the management of prostate cancer in a contemporary cohort. *Cancer* 2008; 112:2664–2670.
48. Conti SL, Dall'era M, Fradet V, Cowan JE, Simko J, Carroll PR. Pathological outcomes of candidates for active surveillance of prostate cancer. *Curr Opin Urol* 2009; 19:258–262.
49. Klotz L. Active surveillance for prostate cancer: trials and tribulations. *World J Urol* 2008; 26:437–442.
50. Adolfsson J. Watchful waiting and active surveillance: the current position. *BJU Int* 2008; 102:10–14.
51. Stattin P, Holmberg E, Johansson JE, Holmberg L, Adolfsson J, Hugosson J; National Prostate Cancer Register (NPCR) of Sweden. Outcomes in localized prostate cancer: National Prostate Cancer Register of Sweden follow-up study. *J Natl Cancer Inst* 2010; 102:950–958.
52. Klotz L, Zhang L, Lam A, Nam R, Mamedov A, Loblaw A. Clinical results of long-term follow-up of a large, active surveillance cohort with localized prostate cancer. *J Clin Oncol* 2010; 28:126–131.
53. Cabrera AR, Coakley FV, Westphalen AC, et al. Prostate cancer: is inapparent tumor at endorectal MR and MR spectroscopic imaging a favorable prognostic finding in patients who select active surveillance? *Radiology* 2008; 247:444–450.
54. van As NJ, de Souza NM, Riches SF, et al. A study of diffusion-weighted magnetic resonance imaging in men with untreated localised prostate cancer on active surveillance. *Eur Urol* 2009; 56:981–987.
55. Han M, Partin AW, Zahurak M, Piantadosi S, Epstein JI, Walsh PC. Biochemical (prostate specific antigen) recurrence probability following radical prostatectomy for clinically localized prostate cancer. *J Urol* 2003; 169:517–523.
56. Catalona WJ, Smith DS. 5-year tumor recurrence rates after anatomical radical retropubic prostatectomy for prostate cancer. *J Urol* 1994; 152:1837–1842.
57. Kattan MW, Wheeler TM, Scardino PT. Postoperative nomogram for disease recurrence after radical prostatectomy for prostate cancer. *J Clin Oncol* 1999; 17:1499–1507.
58. Zincke H, Oesterling JE, Blute ML, Bergstrahl EJ, Myers RP, Barrett DM. Long-term (15 years) results after radical prostatectomy for clinically localized (stage T2c or lower) prostate cancer. *J Urol* 1994; 152:1850–1857.
59. Silverman JM, Krebs TL. MR imaging evaluation with a transrectal surface coil of local recurrence of prostatic cancer in men who have undergone radical prostatectomy. *AJR Am J Roentgenol* 1997; 168:379–385.
60. Sella T, Schwartz LH, Swindle PW, et al. Suspected local recurrence after radical prostatectomy: endorectal coil MR imaging. *Radiology* 2004; 231:379–385.
61. Cirillo S, Petracchini M, Scotti L, et al. Endorectal magnetic resonance imaging at 1.5 Tesla to assess local recurrence following radical prostatectomy using T2-weighted and contrast-enhanced imaging. *Eur Radiol* 2009; 19:761–769.
62. Kuban DA, Thames HD, Levy LB, et al. Long-term multi-institutional analysis of stage T1-T2 prostate cancer treated with radiotherapy in the PSA era. *Int J Radiat Oncol Biol Phys* 2003; 57:915–928.
63. Pucar D, Shukla-Dave A, Hricak H, et al. Prostate cancer: correlation of MR imaging and MR spectroscopy with pathologic findings after radiation therapy-initial experience. *Radiology* 2005; 236:545–553.
64. Sala E, Eberhardt SC, Akin O, et al. Endorectal MR imaging before salvage prostatectomy: tumor localization and staging. *Radiology* 2006; 238:176–183.
65. Arumainayagam N, Kumaar S, Ahmed HU, et al. Accuracy of multiparametric magnetic resonance imaging in detecting recurrent prostate cancer after radiotherapy. *BJU Int* 2010; 106:991–997.
66. Yakar D, Hambrick T, Huisman H, et al. Feasibility of 3T dynamic contrast-enhanced magnetic resonance-guided biopsy in localizing local recurrence of prostate cancer after external beam radiation therapy. *Invest Radiol* 2010; 45:121–125.